CHEMPHYSCHEM

Supporting Information

SUPPORTING INFORMATION

Role of Excited States in Low Energy Electron (LEE) Induced Strand Breaks in DNA Model Systems: Influence of Aqueous Environment

Anil Kumar and Michael D. Sevilla
Department of Chemistry
Oakland University, Rochester
MI 48309

Table T1- Vertical Excitation Energies (ΔE, eV) of Transient Negative Ion (TNI) of DNA/RNA Bases Calculated Using TD-B3LYP/6-31G* and TD-BH&HLYP/6-31G* Methods and Their Comparison with Available Experimental Values[a]

		ΔE		
transition	molecule	B3LYP	BH&HLYP	Exp[b,c]
	uracil			0.22 (π_1*)
$\pi \rightarrow \pi^*$		1.33	1.85	1.58 (π_2*)
$\pi \rightarrow \pi^*$		4.27	4.73	3.83 (π_3*)
	thymine			0.29 (π_1*)
$\pi \rightarrow \pi^*$		1.38	1.89	1.71 (π_2*)
$\pi \rightarrow \pi^*$		3.86	4.46	4.05 (π_3*)
	cytosine			0.32 (π_1*)
$\pi \rightarrow \pi^*$		1.55	1.91	1.53 (π_2*)
$\pi \rightarrow \pi^*$		4.47	5.06	4.50 (π_3*)
	adenine			0.54 (π_1*)
$\pi \rightarrow \pi^*$		0.88	1.0	1.36 (π_2*)
$\pi \rightarrow \pi^*$		1.89	1.86	2.17 (π_3*)
	5′-dTMPH[d]			(0.53 T)[d]
$\pi \rightarrow \pi^*$		1.16	1.68	(1.56 T)[d]
$\pi \rightarrow \sigma^*$[e]		0.18	1.42	(1.80 PO_4)[d]
$\pi \rightarrow \sigma^*$[e]		0.70	2.06	(2.23 S)[d]

[a] Transition energies of radical anions were calculated at the optimized neutral geometry of the molecules. [b] Energies of the shape resonances in the electron transmission spectroscopy (ETS) experiment; ref 15a. [c] π_1* corresponds to the energy of the singly occupied molecular orbital (SOMO), and its difference with π_2* and π_3* orbital energies gives the estimate of the transition energies. [d] Scaled B3LYP orbital energies (VOE); ref 6. [e] Electron transfers from thymine (π) to PO_4 and sugar (σ) part of 5′-dTMPH.

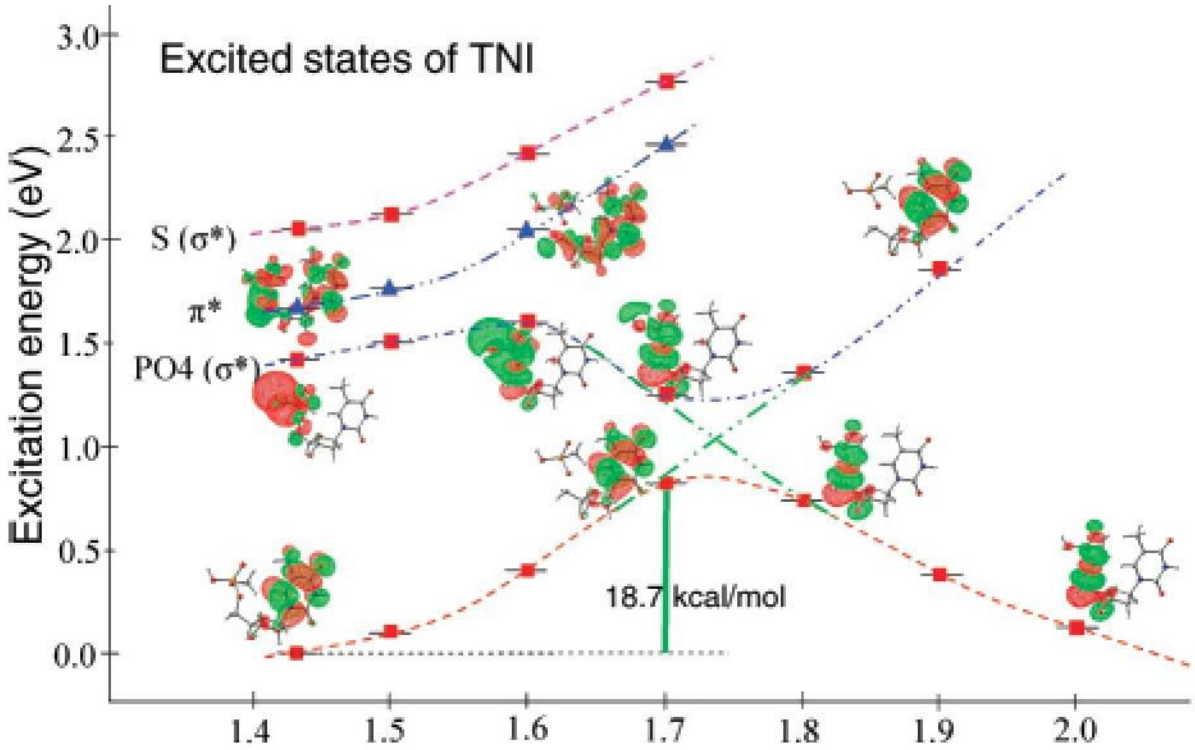

Figure X1- Lower curve: Potential energy surface (PES) of the 5′-dTMPH transient negative ion (TNI); calculated in the neutral optimized geometry of 5′-dTMPH with $C_{5'}$-$O_{5'}$ bond elongation. SOMO is shown at selected points. Upper curves: calculated vertical excitation energies of the radical anion at each point along the PES, MOs involved in excitations are also shown. Energies and distances are given in eV and Å, respectively. The lowest $\pi\pi^*$ state (triangles) and lowest $\pi\sigma^*$ states (square) are shown.

(Reprinted with permission from Ref. 14, J. *Am. Chem. Soc.* © (2008) American Chemical Society.)

(Complete List of Supporting Information)

Table 1- BHandHLYP/6-31G* computed transition energies (eV) of $\pi \rightarrow \sigma(5'\text{-}PO_4)^*$ and $\pi \rightarrow \sigma(3'\text{-}PO_4)^*$ excited states of nucleotides in their adiabatic states in the presence of different environment. A plot between transition energy and different environment is shown in Figure A7.

Table 2- Transition energies (eV) of $\pi \rightarrow \sigma(5'\text{-}PO_4)^*$ and $\pi \rightarrow \sigma(3'\text{-}PO_4)^*$ excited states of nucleotides in their transient negative ion (TNI) states in the presence of different environment. A plot between transition energy and different environment is shown in Figure A8.

Complete Reference 15.

Figure A1- B3LYP/6-31G* optimized structures of 2'-deoxyguanosine-3',5'-diphosphate (3',5'-dGDP) and 2'-deoxyadenosine-3',5'-diphosphate (3',5'-dADP) radical anions in gas phase and in the presence of three water molecules.

Figure A2- B3LYP/6-31G* optimized structures of 2'-deoxythymidine-3',5'-diphosphate (3',5'-dTDP) and 2'-deoxycytidine-3',5'-diphosphate (3',5'-dCDP) radical anions in gas phase and in the presence of two water molecules.

Figure V1- TD-BHandHLYP/6-31G(d) computed transition energies of 3',5'-$dT^{\bullet-}DP$ in gas phase and aqueous solution of the transient negative ion (TNI). The effect of bulk water solvent was considered using IEF-PCM model on the hydrated (3',5'-$dT^{\bullet-}DP + 3H_2O$) system. Transition occurring from SOMO to different MOs (**shape resonance**) is shown. Transition energies are given in eV. The transition energies of TNI were calculated at the optimized geometries of the neutral systems.

Figure V2- TD-BHandHLYP/6-31G(d) computed transition energies of 3',5'-$dC^{\bullet-}DP$ in gas phase and aqueous solution of the transient negative ion (TNI). The effect of bulk water solvent was considered using IEF-PCM model on the hydrated (3',5'-$dC^{\bullet-}DP + 3H_2O$) system. Transition occurring from SOMO to different MOs (**shape resonance**) is shown. Transition energies are given in eV. The transition energies of TNI were calculated at the optimized geometries of the neutral systems.

Figure V3- TD-BHandHLYP/6-31G(d) computed transition energies of 3',5'-$dG^{\bullet-}DP$ in gas phase and aqueous solution of the transient negative ion (TNI). The effect of bulk water solvent was considered using IEF-PCM model on the hydrated (3',5'-$dA^{\bullet-}DP + 3H_2O$) system. Transition occurring from SOMO to different MOs (**shape resonance**) is shown. Transition energies are given in eV. The transition energies of TNI were calculated at the optimized geometries of the neutral systems.

Figure V4- TD-BHandHLYP/6-31G(d) computed transition energies of 3',5'-$dA^{\bullet-}DP$ in gas phase and aqueous solution of the transient negative ion (TNI). The effect of bulk water solvent was considered using IEF-PCM model on the hydrated (3',5'-$dG^{\bullet-}DP + 3H_2O$) system. Transition occurring from SOMO to different MOs (**shape resonance**) is shown. Transition energies are given in eV. The transition energies of TNI were calculated at the optimized geometries of the neutral systems.

Figure A3- TD-BHandHLYP/6-31G* computed transition energies of 3',5'-$dG^{\bullet-}DP$ in gas phase and aqueous solution.

Figure A4- TD-BHandHLYP/6-31G* computed transition energies of 3',5'-$dT^{\bullet-}DP$ in gas phase and aqueous solution.

Figure A5- TD-BHandHLYP/6-31G(d) computed transition energies of 3',5'-dC$^{\bullet-}$DP in gas phase and aqueous solution.

Figure A6- TD-BHandHLYP/6-31G* computed transition energies of 3',5'-dA$^{\bullet-}$DP in gas phase and aqueous solution.

Figure A7- Variation of transition energies (eV) of $\pi\rightarrow\sigma(5'\text{-}PO_4)^*$ (left) and $\pi\rightarrow\sigma(3'\text{-}PO_4)^*$ (right) excited states of nucleotides in their adiabatic states with increasing solvation. Different solvation levels labeled on X-axis are: 1- gas phase, 2- three discrete water molecules , 3- three waters and a continuous dielectric ($\varepsilon = 7.0$) and 4- three waters and a continuous dielectric ($\varepsilon = 78.4$).

Figure A8- Variation of transition energies (eV) of $\pi\rightarrow\sigma(5'\text{-}PO_4)^*$ (left) and $\pi\rightarrow\sigma(3'\text{-}PO_4)^*$ (right) excited states of nucleotides in their TNI states with increasing solvation. Different solvation levels labeled on X-axis are: 1- gas phase, 2- three discrete water molecules , 3- three waters and a continuous dielectric ($\varepsilon = 7.0$) and 4- three waters and a continuous dielectric ($\varepsilon = 78.4$).

Table 1- Transition energies (eV) of $\pi\rightarrow\sigma(5'\text{-}PO_4)^*$ and $\pi\rightarrow\sigma(3'\text{-}PO_4)^*$ excited states of di nucleotides in their adiabatic states in the presence of different environment. A plot between transition energy and different environment is shown in Figure A7.

Molecule[a]	Location of σ*- orbital	Transition energy (eV)			
		Gas phase	Discrete Water[a] (Without PCM)	Water with PCM (ε=7.0)	Water with PCM (ε=78.39)
3',5'-dA$^{\bullet-}$DP	5'-PO_4	2.71	3.55	4.30	4.45
	3'-PO_4	2.97	3.67	4.46	4.60
3',5'-dG$^{\bullet-}$DP	5'-PO_4	3.37	4.19	5.21	5.42
	3'-PO_4	3.42	4.28	5.34	5.55
3',5'-dT$^{\bullet-}$DP	5'-PO_4	3.29	3.55	4.56	4.76
	3'-PO_4	3.50	3.90	4.98	5.19
3',5'-dC$^{\bullet-}$DP	5'-PO_4	3.28	3.62	4.40	4.55
	3'-PO_4	3.62	4.02	4.89	5.06

[a]See Figures A1 and A2**.**

Table 2- Transition energies (eV) of $\pi \rightarrow \sigma(5'\text{-}PO_4)^*$ and $\pi \rightarrow \sigma(3'\text{-}PO_4)^*$ excited states of di nucleotides in their transient negative ion (TNI) states in the presence of different environment. A plot between transition energy and different environment is shown in Figure A8.

Molecule[a]	Location of σ*- orbital	Transition energy (eV)			
		Gas phase	Discrete Water[a] (Without PCM)	Water with PCM (ε=7.0)	Water with PCM (ε=78.39)
3',5'-dA$^{\bullet-}$DP	5'-PO_4	1.14	1.54	2.80	3.11
	3'-PO_4	1.07	1.73	3.14	3.44
3',5'-dG$^{\bullet-}$DP	5'-PO_4	0.46	1.49	2.88	3.18
	3'-PO_4	0.35	1.29	2.85	3.20
3',5'-dT$^{\bullet-}$DP	5'-PO_4	1.18	1.33	3.02	3.40
	3'-PO_4	1.46	1.85	3.47	3.82
3',5'-dC$^{\bullet-}$DP	5'-PO_4	1.25	1.27	2.86	3.22
	3'-PO_4	1.66	1.62	3.19	3.53

Complete Reference 15

M.J. Frisch, G.W. Trucks, H.B. Schlegel, G.E. Scuseria, M.A. Robb, J.R. Cheesemean, J.J.A. Montogomery, T. Vreven, K.N. Kudin, J.C. Burant, J.M. Millam, S.S. Iyengar, J. Tomasi, V. Barone, B. Mennucci, M. Cossi, G.Scalmani, N. Rega, G.A. Petersson, H. Nakatsuji, M. Hada, M. Ehara, K. Toyota, R. Fukuda, J. Hasegawa, M. Ishida, T. Nakajima, Y. Honda, O, Kitao, H. Nakai, M. Klene, X. Li, J.E. Knox, H.P. Hratchian, J.B. Cross, V. Bakken, C. Adamo, J. Jaramillo, R. Gomperts, R.E. Stratmann, O. Yazyev, A.J. Austin, R. Cammi, C. Pomelli, J.W. Ochtersk, P.Y. Ayala, K. Morokuma, G.A. Voth, P. Salvador, J.J. Dannenberg, V.G. Zakrzewski, S. Dapprich, A.D. Daniels, M.C. Strain, O. Farkas, D.K. Malick, A.D. Rabuck, K. Raghavachari, J.B. Foresman, J.V. Oritz, Q. Cui, A.G. Baboul, S. Clifford, J. Cioslowski, B.B. Stefanov, G. Liu, A. Liashenko, P. Piskorz, I. Komaromi, R.L. Martin, D.J. Fox, T. Keith, M.A. Al-Laham, C.Y. Peng, A. Nanayakkara, M. Challacombe, P.M.W. Gill, B. Johnson, W. Chen, M.W. Wong, C. Gonzalez, and J. A. Pople, *GAUSSIAN 03* (Rev. C.02), Gaussian Inc, Wallingford, CT, 2004.

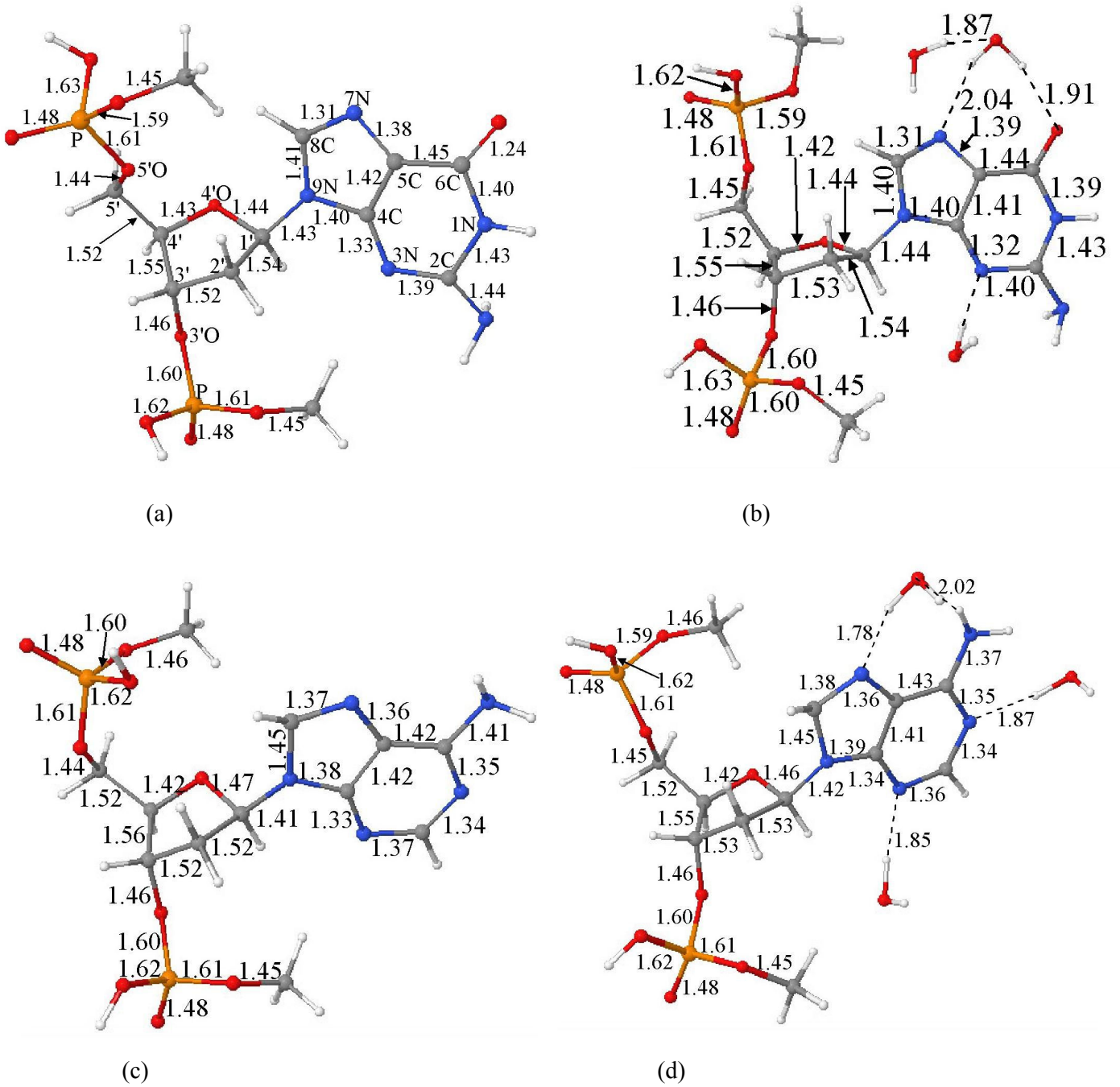

Figure A1- B3LYP/6-31G* optimized structures of 2'-deoxyguanosine-3',5'-diphosphate (3',5'-dGDP) and 2'-deoxyadenosine-3',5'-diphosphate (3',5'-dADP) radical anions in gas phase and in the presence of three water molecules. Bond lengths are given in angstroms (Å). The atom numbers of purine base, sugar and phosphate are also shown in (a).

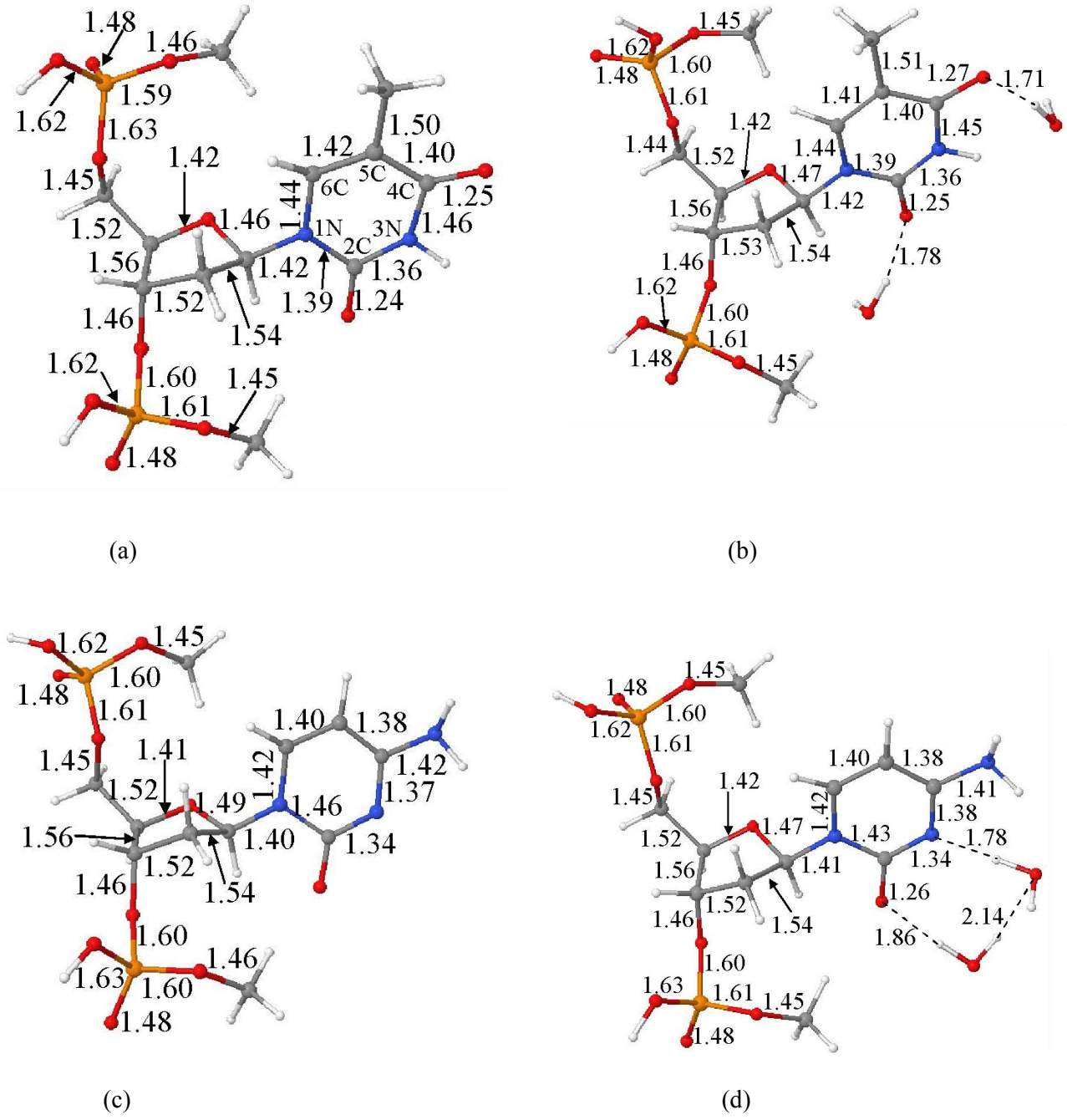

Figure A2- B3LYP/6-31G* optimized structures of 2'-deoxythymidine-3',5'-diphosphate (3',5'-dTDP) and 2'-deoxycytidine-3',5'-diphosphate (3',5'-dCDP) radical anions in gas phase and in the presence of two water molecules. Bond lengths are given in angstroms (Å). The atom numbers of pyrimidine base are also shown in (a).

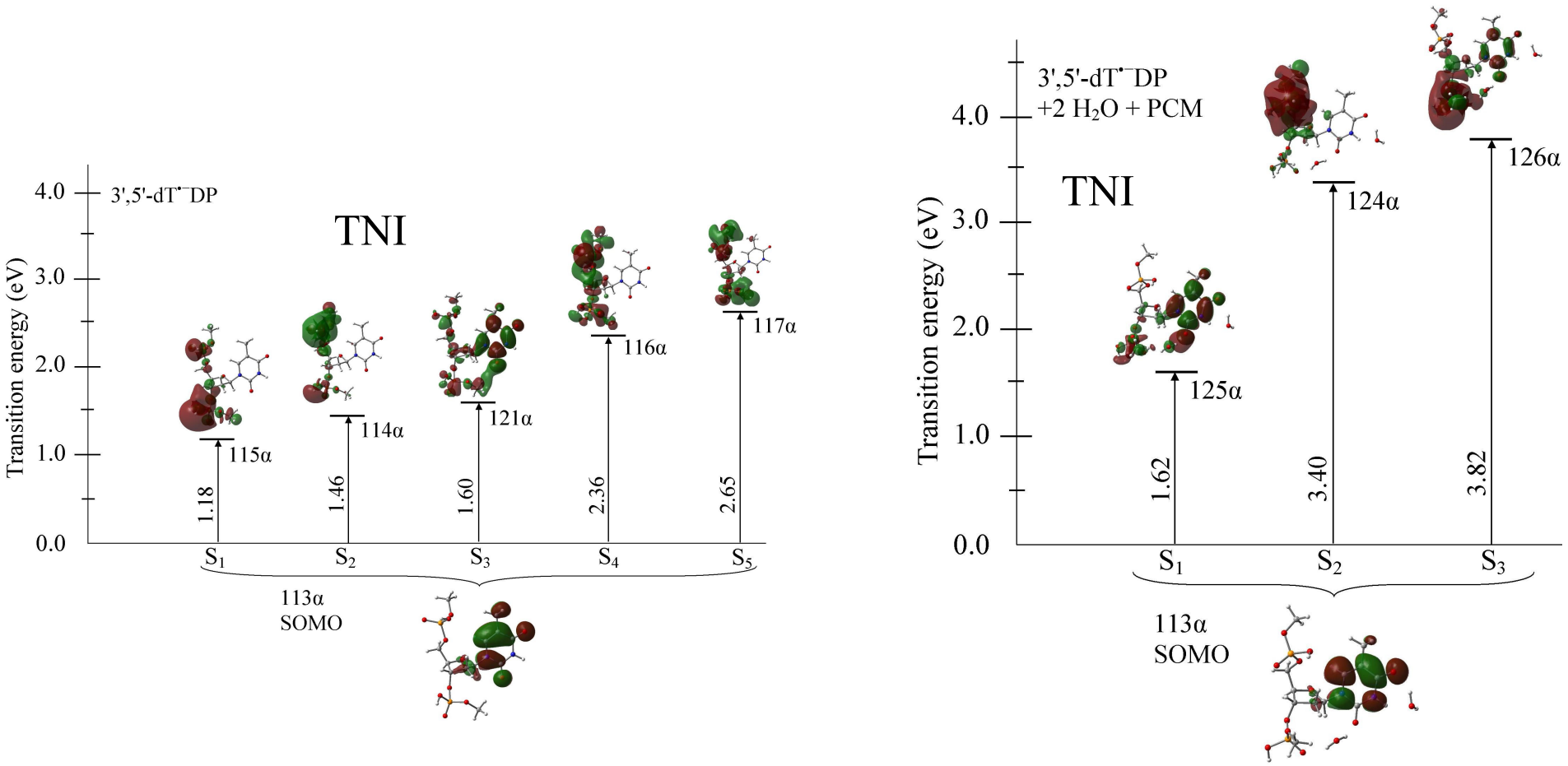

Figure V1- TD-BHandHLYP/6-31G(d) computed transition energies of 3',5'-dT•⁻DP in gas phase and aqueous solution of the transient negative ion (TNI). The effect of bulk water solvent was considered using IEF-PCM model on the hydrated (3',5'-dT•⁻DP + $3H_2O$) system. Transition occurring from SOMO to different MOs (**shape resonance**) is shown. Transition energies are given in eV. The transition energies of TNI were calculated at the optimized geometries of the neutral systems.

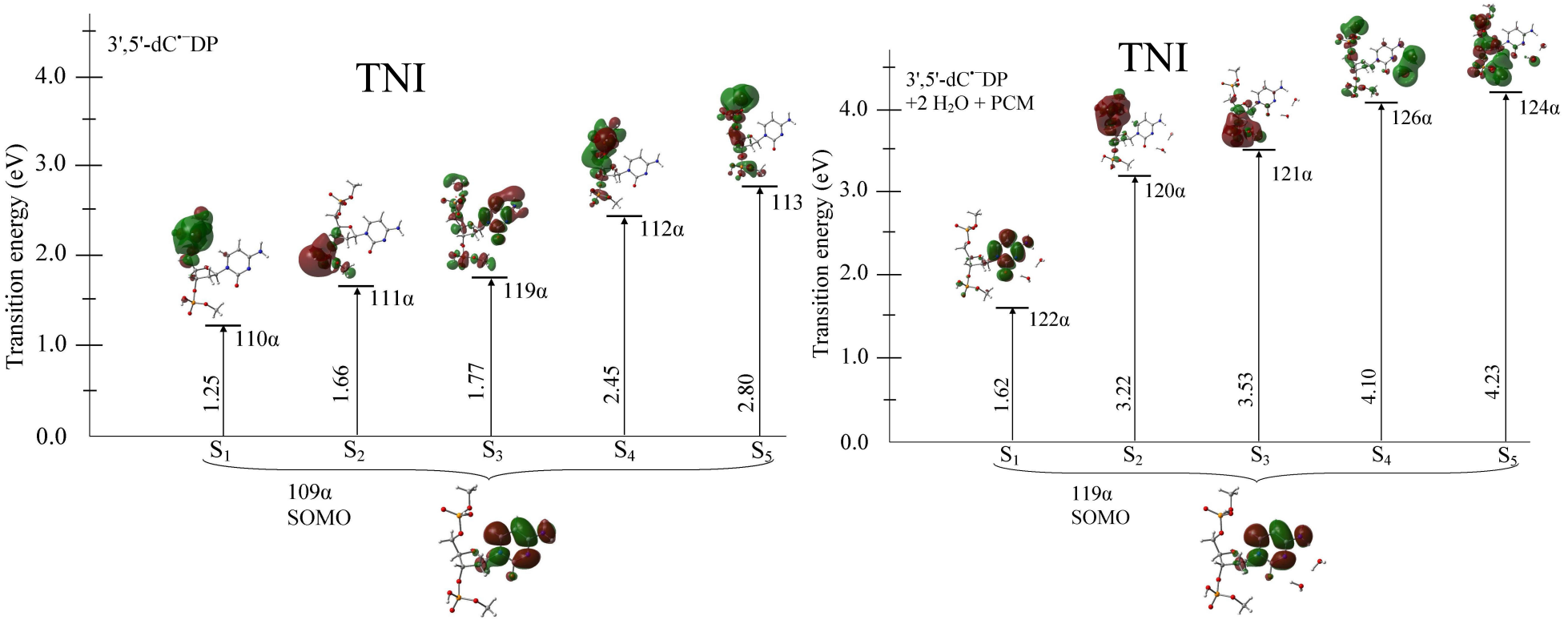

Figure V2- TD-BHandHLYP/6-31G(d) computed transition energies of 3',5'-dC•⁻DP in gas phase and aqueous solution of the transient negative ion (TNI). The effect of bulk water solvent was considered using IEF-PCM model on the hydrated (3',5'-dC•⁻DP + $3H_2O$) system. Transition occurring from SOMO to different MOs (**shape resonance**) is shown. Transition energies are given in eV. The transition energies of TNI were calculated at the optimized geometries of the neutral systems.

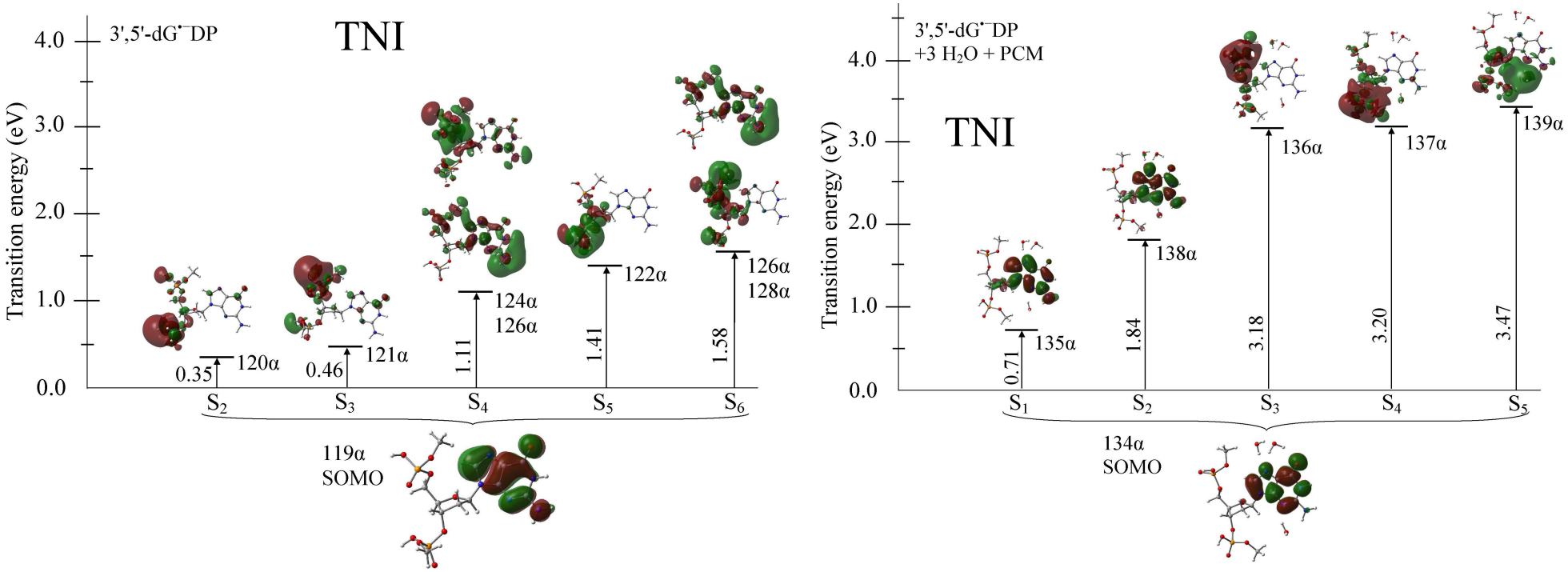

Figure V3- TD-BHandHLYP/6-31G(d) computed transition energies of 3',5'-dG•⁻DP in gas phase and aqueous solution of the transient negative ion (TNI). The effect of bulk water solvent was considered using IEF-PCM model on the hydrated (3',5'-dG•⁻DP + $3H_2O$) system. Transition occurring from SOMO to different MOs (**shape resonance**) is shown. Transition energies are given in eV. The transition energies of TNI were calculated at the optimized geometries of the neutral systems.

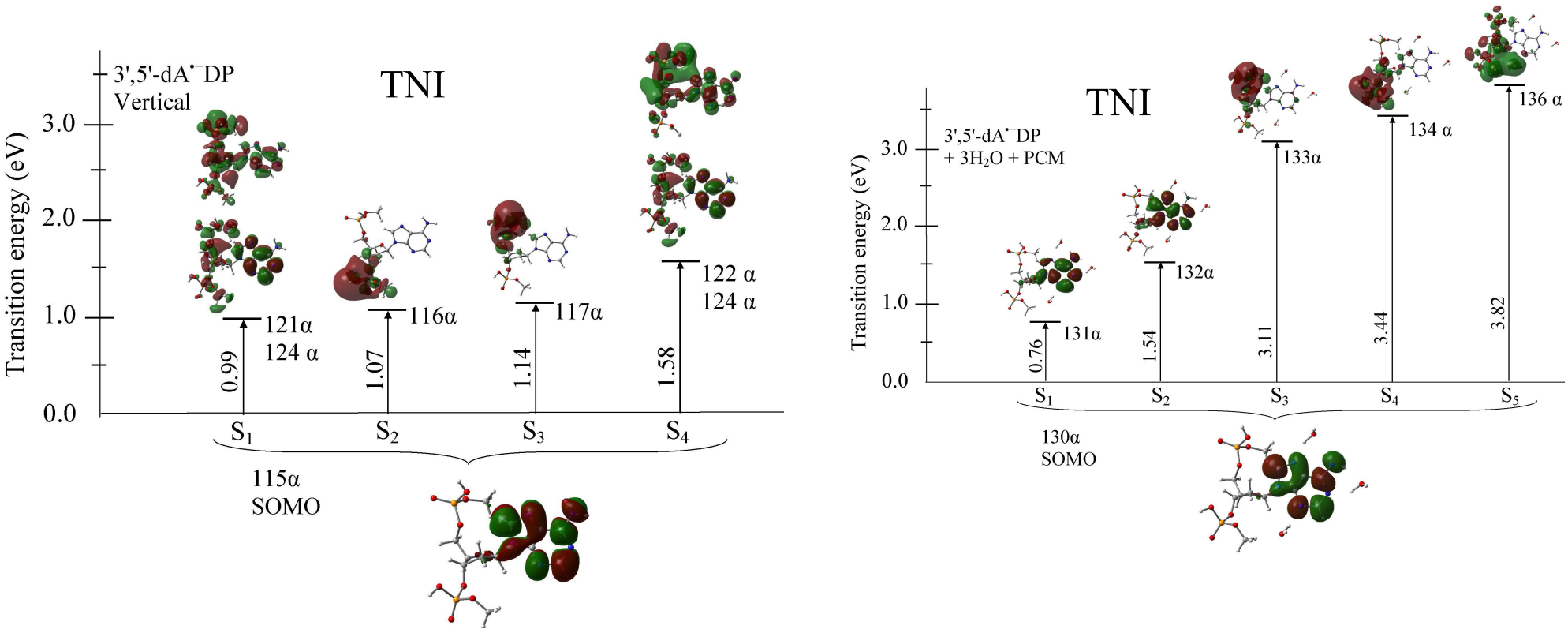

Figure V4- TD-BHandHLYP/6-31G(d) computed transition energies of 3',5'-dA•⁻DP in gas phase and aqueous solution of the transient negative ion (TNI). The effect of bulk water solvent was considered using IEF-PCM model on the hydrated (3',5'-dA•⁻DP + $3H_2O$) system. Transition occurring from SOMO to different MOs (**shape resonance**) is shown. Transition energies are given in eV. The transition energies of TNI were calculated at the optimized geometries of the neutral systems.

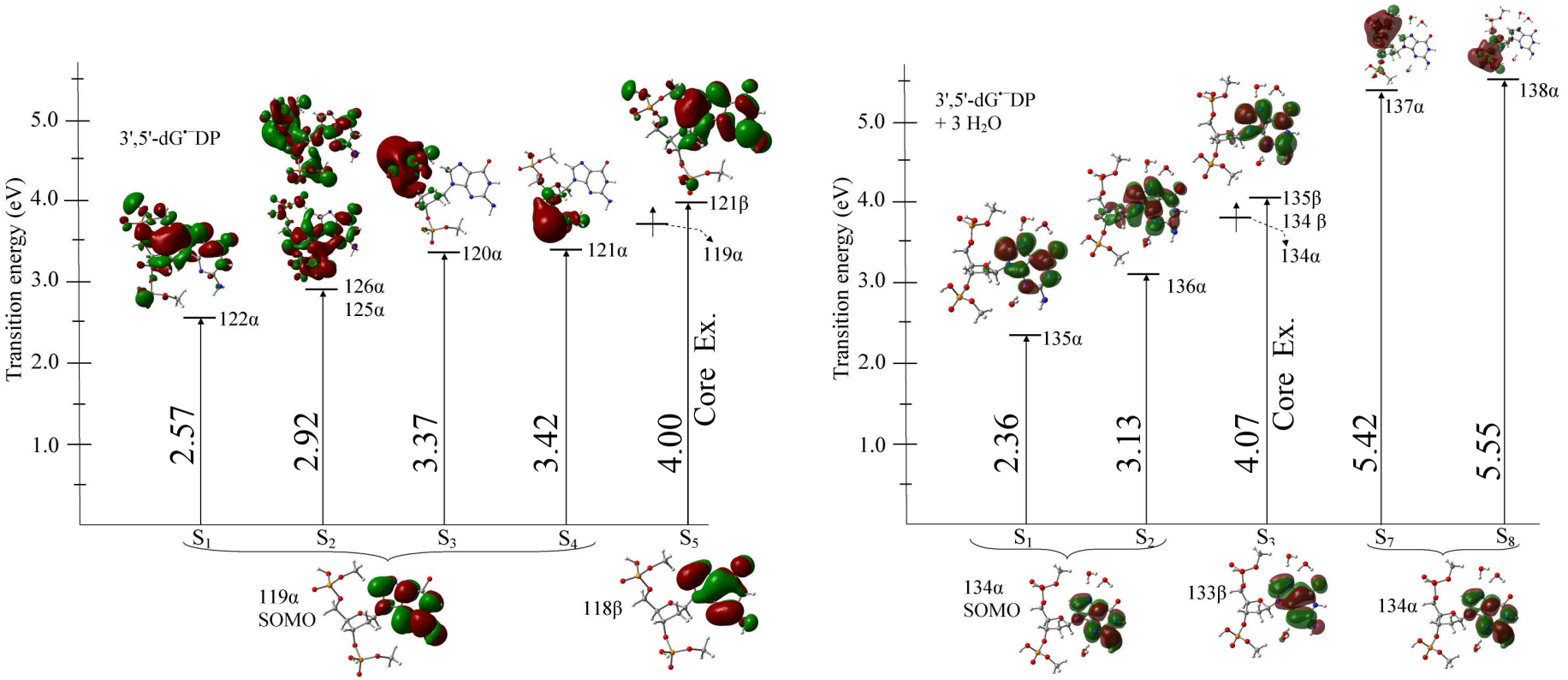

Figure A3- TD-BHandHLYP/6-31G(d) computed transition energies of 3',5'-dG$^{\bullet-}$DP in gas phase and aqueous solution. The effect of bulk water solvent was considered using IEF-PCM model on the hydrated (3',5'-dG$^{\bullet-}$DP + 3H_2O). Transition occurs from SOMO to different MOs and from inner shell to different MOs (**core excitation**) is shown. Transition energies are given in eV.

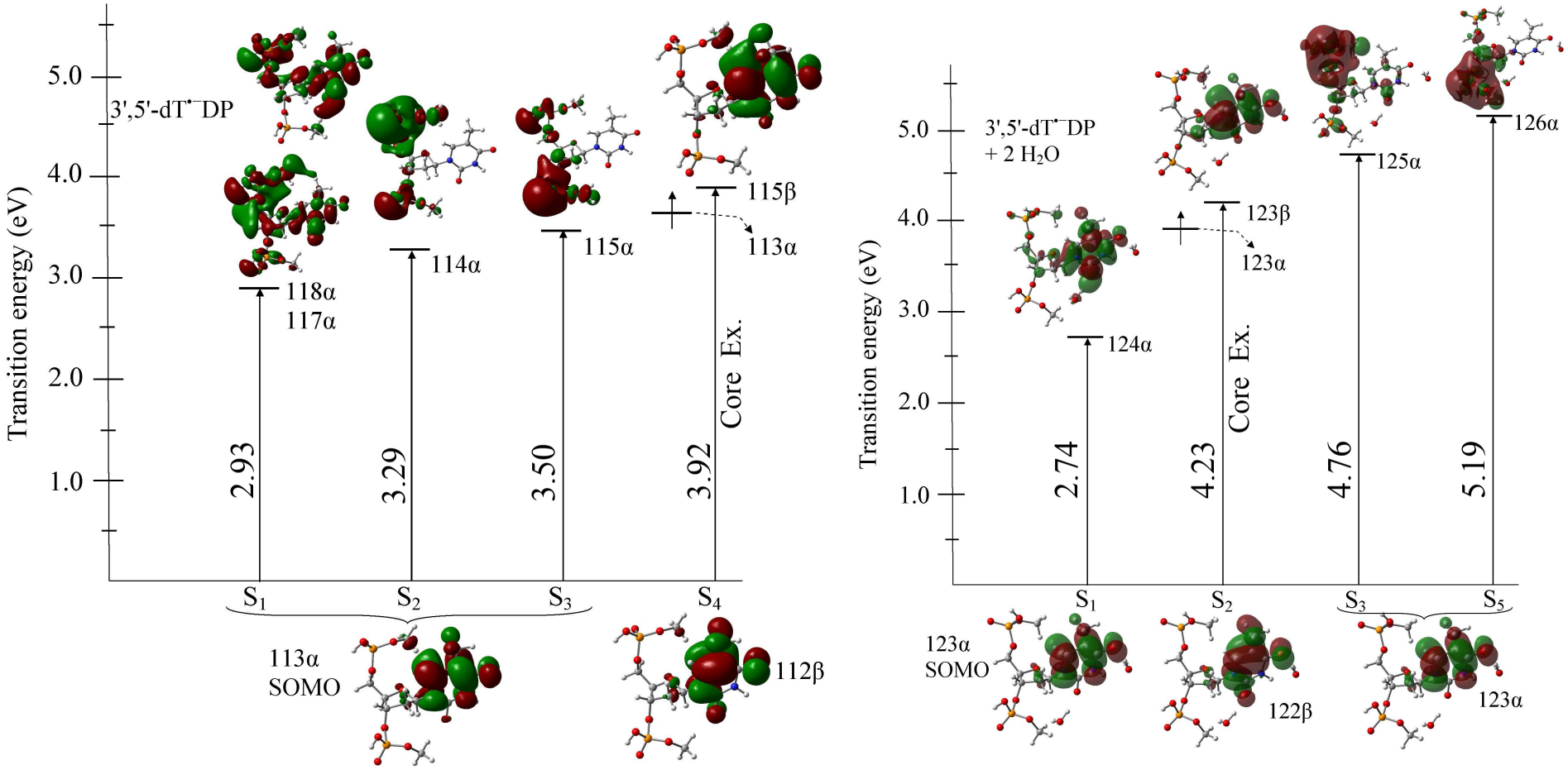

Figure A4- TD-BHandHLYP/6-31G* computed transition energies of 3',5'-dT•⁻DP in gas phase and aqueous solution. The effect of bulk water solvent was considered using IEF-PCM model on the hydrated 3',5'-dT•⁻DP system. Transition occurs from SOMO to different MOs and from inner shell to different MOs (**core excitation**) is shown. Transition energies are given in eV.

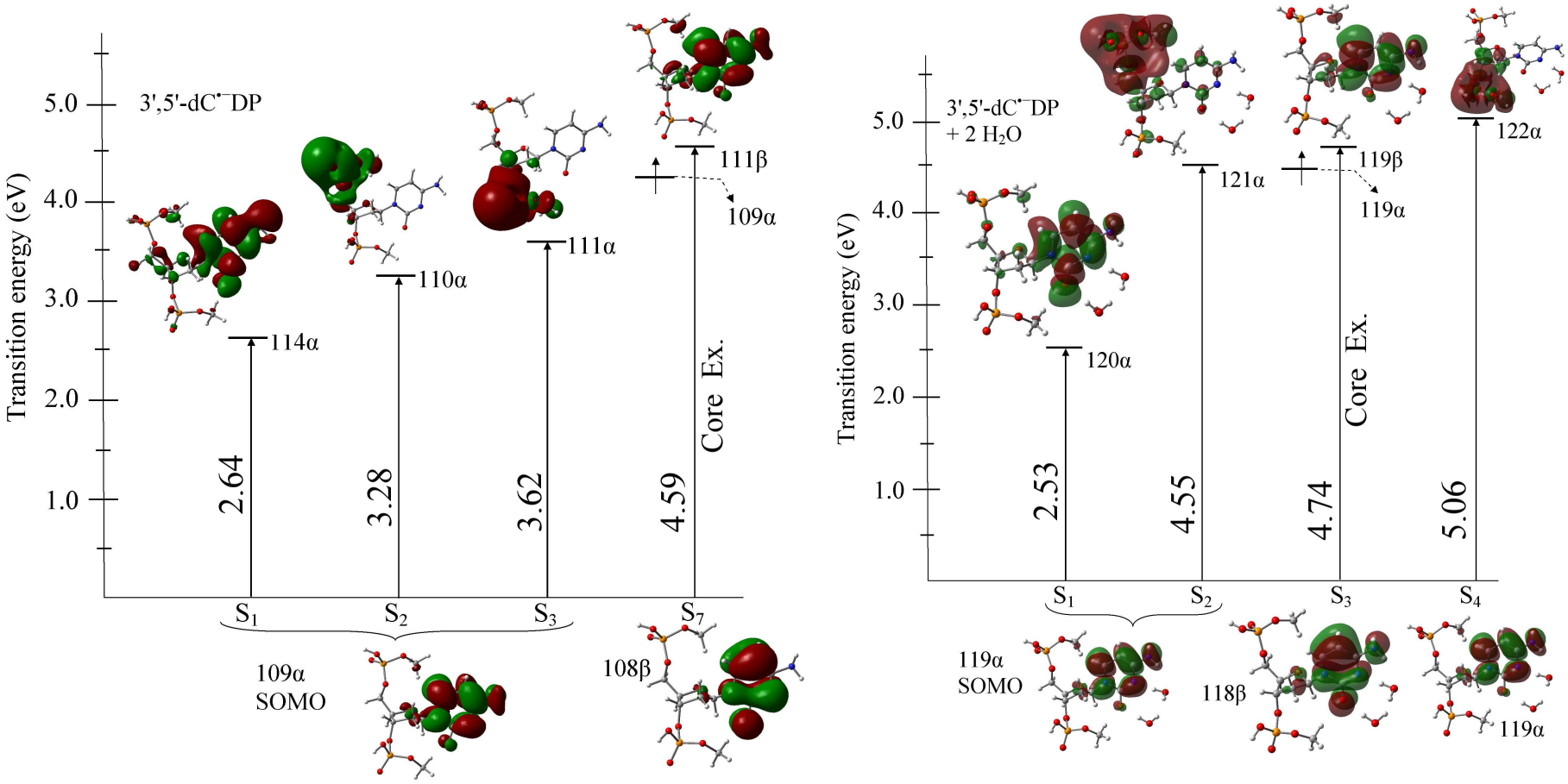

Figure A5- TD-BHandHLYP/6-31G(d) computed transition energies of 3',5'-dC•⁻DP in gas phase and aqueous solution. The effect of bulk water solvent was considered using IEF-PCM model on the hydrated 3',5'-dC•⁻DP system. Transition occurs from SOMO to different MOs and from inner shell to different MOs (**core excitation**) is shown. Transition energies are given in eV.

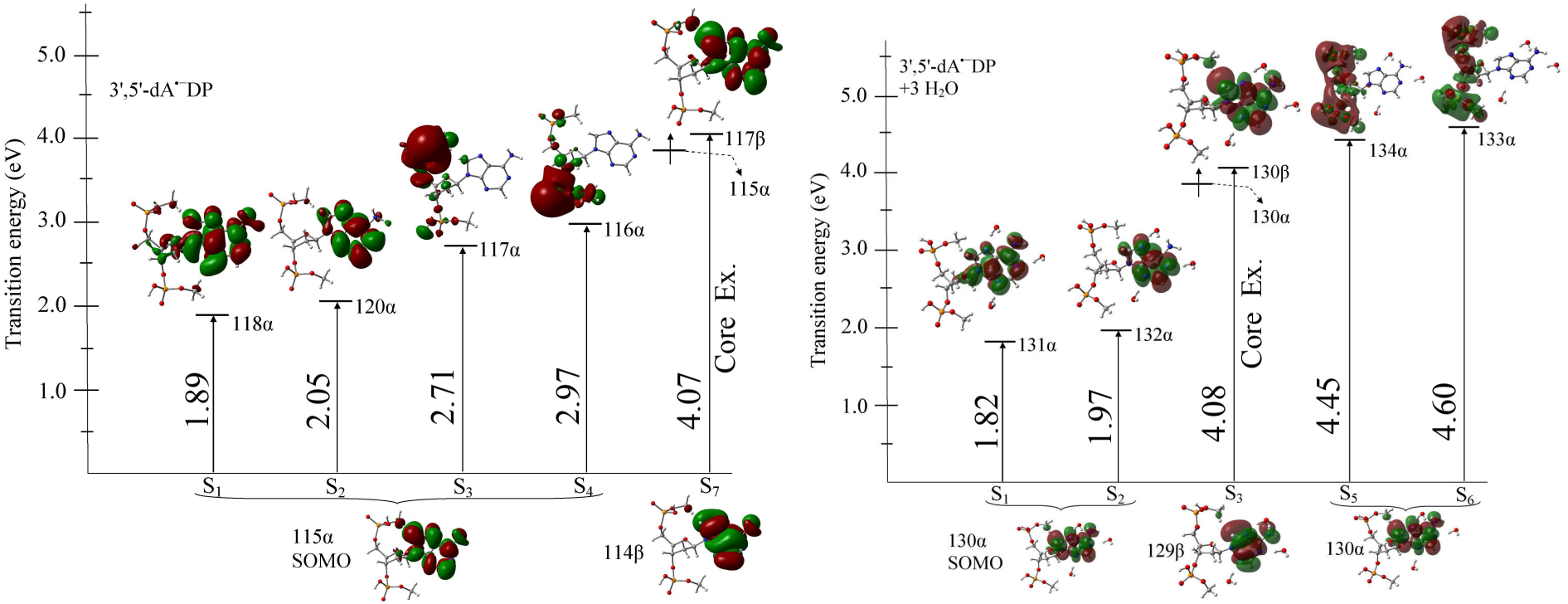

Figure A6- TD-BHandHLYP/6-31G(d) computed transition energies of 3',5'-dA$^{\bullet-}$DP in gas phase and aqueous solution. The effect of bulk water solvent was considered using IEF-PCM model on the hydrated (3',5'-dA$^{\bullet-}$DP + 2H_2O) system. Transition occurs from SOMO to different MOs and from inner shell to different MOs (**core excitation**) is shown. Transition energies are given in eV.

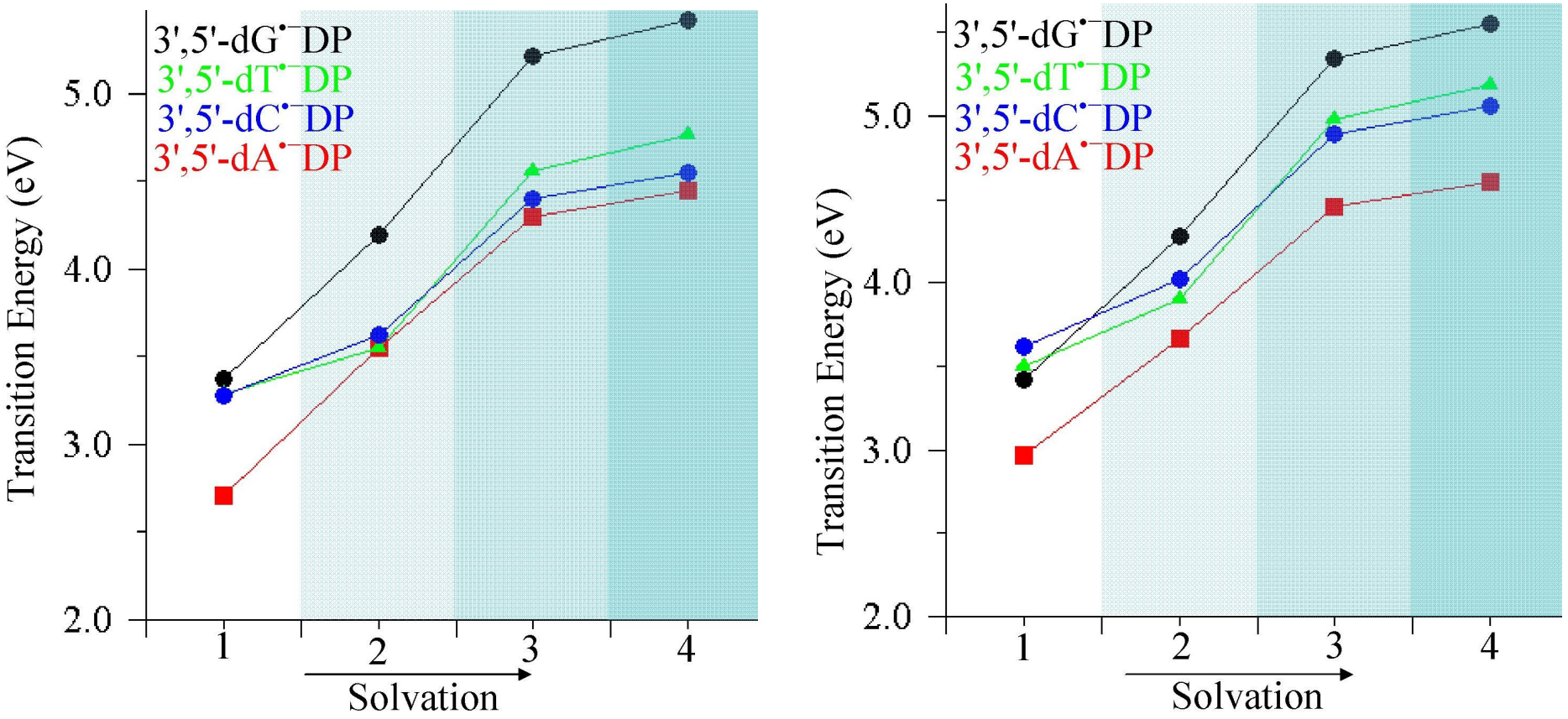

Figure A7- Variation of transition energies (eV) of $\pi \rightarrow \sigma(5'\text{-}PO_4)^*$ (left) and $\pi \rightarrow \sigma(3'\text{-}PO_4)^*$ (right) excited states of nucleotides in their adiabatic states with increasing solvation. Different solvation levels labeled on X-axis are: 1- gas phase, 2- three discrete water molecules , 3- three waters and a continuous dielectric ($\varepsilon = 7.0$) and 4- three waters and a continuous dielectric ($\varepsilon = 78.4$).

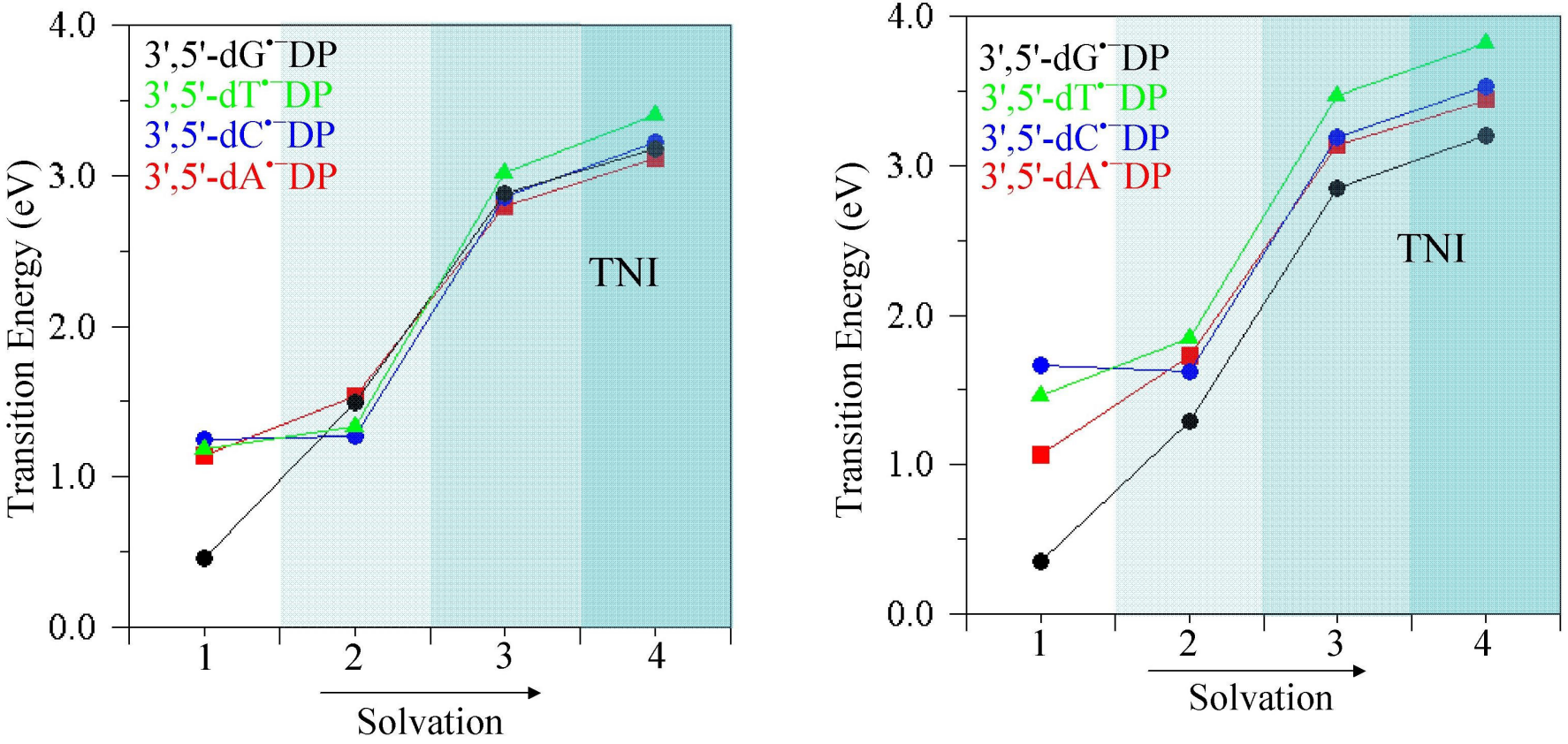

Figure A8- Variation of transition energies (eV) of $\pi \rightarrow \sigma(5'\text{-}PO_4)^*$ (left) and $\pi \rightarrow \sigma(3'\text{-}PO_4)^*$ (right) excited states of nucleotides in their TNI states with increasing solvation. Different solvation levels labeled on X-axis are: 1- gas phase, 2- three discrete water molecules , 3- three waters and a continuous dielectric ($\varepsilon = 7.0$) and 4- three waters and a continuous dielectric ($\varepsilon = 78.4$).